Photoelectron and Auger-electron spectra of Cl3SiSi(CH3)3 obtained by using monochromatized synchrotron radiation

ARTICLE *in* JOURNAL OF ELECTRON SPECTROSCOPY AND RELATED PHENOMENA · AUGUST 2014

Impact Factor: 1.44 · DOI: 10.1016/j.elspec.2014.04.009

6 AUTHORS, INCLUDING:

Isao H Suzuki

High Energy Accelerator Research Organiza…

191 PUBLICATIONS **2,145** CITATIONS

Journal of Electron Spectroscopy and Related Phenomena 195 (2014) 18–25

Contents lists available at ScienceDirect

Journal of Electron Spectroscopy and Related Phenomena

journal homepage: www.elsevier.com/locate/elspec

Photoelectron and Auger-electron spectra of $Cl_3SiSi(CH_3)_3$ obtained by using monochromatized synchrotron radiation

Shin-ichi Nagaoka[a,*], Hikaru Endo[a], Kanae Nagai[a], Osamu Takahashi[b], Yusuke Tamenori[c], Isao H. Suzuki[d,e]

[a] Department of Chemistry, Faculty of Science and Graduate School of Science and Engineering, Ehime University, Matsuyama 790-8577, Japan
[b] Institute for Sustainable Sciences and Development, Hiroshima University, Higashi-Hiroshima 739-8511, Japan
[c] Synchrotron Radiation Research Institute/SPring-8, 1-1-1 Kouto, Sayo-cho, Sayo-gun 679-5198, Japan
[d] Institute of Materials Structure Science, High Energy Accelerator Research Organization (KEK), 1-1 Oho, Tsukuba 305-0801, Japan
[e] Advanced Institute of Industrial Science and Technology (AIST), 1-1-1 Umezono, Tsukuba 305-8568, Japan

ARTICLE INFO

Article history:
Received 13 February 2014
Received in revised form 16 April 2014
Accepted 17 April 2014
Available online 26 April 2014

Keywords:
Si-containing molecule
Photoelectron spectroscopy
Auger-electron spectroscopy
Monochromatized synchrotron radiation
Site-specific fragmentation

ABSTRACT

A variety of photoelectron and Auger-electron spectra of 1,1,1-trimethyltrichlorodisilane vapor ($Cl_3SiSi(CH_3)_3$) were measured by using monochromatized synchrotron radiation and a hemispherical electron energy analyzer. The measured spectra were interpreted with the aid of some calculations by means of the outer valence Green's function (OVGF) method or the density-functional-theory (DFT) method. Since $Cl_3SiSi(CH_3)_3$ consists of —$SiCl_3$ and —$Si(CH_3)_3$ moieties, the experimental core-electron binding-energies were compared with those of tetrachlorosilane and tetramethylsilane ($SiCl_4$ and $Si(CH_3)_4$, respectively). This comparison showed that electronic properties of $Cl_3SiSi(CH_3)_3$ hold a close correlation with those of $SiCl_4$ and $Si(CH_3)_4$. Si:L_{23}VV, Cl:L_{23}VV and C:KVV Auger-electron spectra of $Cl_3SiSi(CH_3)_3$ also showed profiles close to those expected from the spectra of $SiCl_4$ and $Si(CH_3)_4$. The results obtained here were discussed in conjunction with electronic relaxation leading to site-specific fragmentation.

1. Introduction

Ionization of a material gives various pieces of information on the electronic structure, and a number of researchers have carried out measurements of photoelectrons and Auger electrons [1–3]. A photoelectron spectrum (PES spectrum) of a molecule provides a binding energy (BE) for the individual orbitals. A valence orbital is composed of higher-lying atomic orbitals, and the BE value is governed by characteristics of these atomic orbitals. The BE value for a core orbital always depends on the chemical environment around the atom to which the orbital originally belonged, and thus a core-electron BE difference between atoms of the same element with differing chemical environment has been recognized as a chemical shift for many years [4]. Therefore, electron spectroscopy has been often utilized as a powerful tool for determination of the chemical shift as well as for clarification of electronic structures [1–3].

It is possible to excite and/or remove (ionize) a core electron at a specified atomic site in a molecule using monochromatized soft X-ray irradiation. Site-specific fragmentation induced by such excitation or ionization has attracted much attention in terms of clarification of dynamical behavior in the excited or ionized molecule, although the core electron does not directly participate in the chemical bonding [5–10]. In particular, Si-containing molecules are interesting in view of industrial application to precise fabrication of electronic devices. Several fragment ions formed through element-specific processes were found in a number of molecules excited and/or ionized by monochromatized synchrotron radiation in the vapor phase [5–7].

Real site-specific fragmentation was discovered in Si core-ionization of 1-trifluorosilyl-2-trimethysilylethane ($F_3SiCH_2CH_2Si(CH_3)_3$, FSMSE) [8–11]. In FSMSE, ionic fragmentation induced by 2p core-ionization at the Si atom bonding to three F atoms (Si[F]) exhibited a feature significantly different from that at the Si bonding to three CH_3 groups (Si[Me]). Since the chemical environment around the Si[F] site is very different from that around Si[Me], the BE value obtained for the Si[F]:2p core orbital was very different from that for the Si[Me]:2p orbital; that is, a large chemical-shift was seen between the Si[F]:2p and

* Corresponding author. Tel.: +81 89 927 9592.
E-mail address: nagaoka@ehime-u.ac.jp (S. Nagaoka).

http://dx.doi.org/10.1016/j.elspec.2014.04.009
0368-2048/

Si[Me]:2p photoelectron peaks. Similar results were obtained in 1-trichlorosilyl-3-trimethylsilylethane ($Cl_3SiCH_2CH_2Si(CH_3)_3$, CSMSE) [10].

On the other hand, in 1,1,1-trimethyltrichlorodisilane ($Cl_3SiSi(CH_3)_3$, MCDS), ionic fragmentation induced by 2p core-ionization at the Si atom bonding to three Cl atoms (Si[Cl]) was similar to that at the Si bonding to three CH_3 groups (Si[Me]) [10,12]. These findings in FSMSE, CSMSE and MCDS seem to be connected with the distance between the two Si atoms and with spatial distribution of valence holes created through Auger decays following the Si:2p ionization. The two Si atoms in MCDS are directly bonded to each other, while each of FSMSE and CSMSE has a dimethylene bridge (—CH_2CH_2—) between the two Si atoms. The origin of the difference in site-specific phenomena between FSMSE (CSMSE) and MCDS may be clarified through precise investigation of the Auger decay processes from the core ionized states. Further, a question happens whether or not ionization of another core electron (C:1s, Cl:1s, 2s, 2p, Si:1s or 2s) yields a behavior different from that of the Si:2p electron in MCDS, while all of the BE values and Auger-electron spectra (AES spectra) were previously determined in FSMSE [13,14].

In order to clarify electronic structures and dynamical behaviors of MCDS, measurements of all the BE values and AES spectra are required. Electron spectroscopic techniques combined with monochromatized synchrotron radiation play significant roles in such a study. Soft X-rays are occasionally useful for determination of BE values of valence electrons, because photoelectron measurements with the aid of soft X-rays are almost free from cross-section variations near ionization thresholds [13]. Furthermore, an AES spectrum obtained through photoexcitation is clearer than those with energetic charged beams, because the background is very low and ionizations with mono-energetic photons allow us to obtain a spectrum originating only from a core-ionized state of interest [14–20].

In the present study, electron emission spectra of MCDS vapor have been measured at several photon energies between 310 and 1950 eV by using an electron spectrometer combined with monochromatized undulator radiation. The measured spectra are interpreted with the aid of some calculations by means of the outer valence Green's function (OVGF) method or the density-functional-theory (DFT) method. Since MCDS consists of —$SiCl_3$ and —$Si(CH_3)_3$ moieties, the core-PES and AES spectra are compared with those of tetrachlorosilane and tetramethylsilane ($SiCl_4$ and $Si(CH_3)_4$, TCS and TMS, respectively). The results obtained here are discussed in conjunction with electronic relaxation leading to site-specific fragmentation.

2. Experimental method and procedures

The molecular structures of MCDS, TCS and TMS are given in Scheme 1. Preparation of MCDS was reported previously [21]. MCDS was degassed by means of the repeated freeze–pump–thaw method prior to measurements. A comparison of PES and AES spectra of MCDS with those of 1,1,1-trimethyltrifluorodisilane ($F_3SiSi(CH_3)_3$) may be informative. However, we could not prepare it because a CH_3 group and a F atom tend to become exchanged.

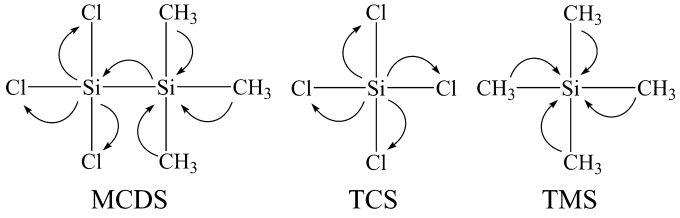

Scheme 1. Structures of molecules discussed in the present work, together with schematic representation of electron-donating and -accepting properties in the molecules.

Measurements for MCDS vapor were performed on c branch of soft X-ray photochemistry beamline 27SU at SPring-8 facility [22,23]. The beamline provides linearly polarized monochromatic light ranging from 0.2 to 2.8 keV, which can ionize every orbital electron except Cl:1s one in MCDS. The energy reading of the monochromator was calibrated with respect to the BE values of Ne:1s and 2s electrons [24]. The photon bandwidth employed was about 0.16 eV in most instances and 0.56 eV in the Si:1s ionization. The intensity of the monochromatized incident photon-beam during the measurements was monitored by collecting the drain current of the post-focusing mirror on the beamline.

The electron spectrometer used here consisted of a hemispherical electron spectrometer (Gammadata Scienta, SES-2002) fitted to a gas cell (GC-50) by way of a multi-element lens in a differentially pumped chamber [25]. MCDS vapor was supplied into the gas cell, and its vapor pressure observed was about 2×10^{-4} Pa in the chamber during the measurements. The electron kinetic-energy bandwidth employed was 0.16 eV, and the emitted electrons were detected at the direction parallel to the photon polarization. The kinetic energy reading of the electron spectrometer was calibrated against the kinetic energies of normal Ar:LMM Auger electrons [1]. In order to unravel complex peak structures in some of the measured PES spectra, we employed a peak-fitting technique, in which Voigt functions were used for individual photoelectron peaks [13].

3. Computational method and procedures

After the geometry of MCDS was optimized (supplementary material [26]), the BE values for the valence orbitals were calculated at the HF/6-311+G** level by using Gaussian 09 program [27]. The BE values below 20 eV were estimated according to the OVGF method [28], which includes effects of electron correlation and reorganization beyond the Hartree–Fock approximation. The pole strength is a measure of how easy it is to make the ionization, with 1.0 as the maximum value [29]. The pole strength obtained by means of the OVGF method, or the square of the pole strength [30], is not necessarily proportional to the ionization efficiency [31].

The BE values for the core orbitals of MCDS were calculated according to a method reported previously [32] by using STOBE-DEMON program [33]. A density-functional-theory (DFT) calculation of the single core-hole state was performed with the ΔKS method [34]. IGLO-III basis sets were used for the core orbitals. The gradient-corrected exchange (PD86) [35] and correlation functional (PD91) [36] by Perdew and Wang were used for the correlation-exchange functional in the DFT calculation. Spin–orbit interaction was not included in the calculation.

The DFT calculation was also used to reproduce the Si:L_{23}VV AES spectrum of MCDS according to a method reported previously [14]. The numbers of the singlet and triplet Si:L_{23}VV-Auger final-states were 325 and 300, respectively, for each of Si[Cl]:2p_x, Si[Cl]:2p_y, Si[Cl]:2p_z, Si[Me]:2p_x, Si[Me]:2p_y and Si[Me]:2p_z core holes. The line spectra showing the individual Auger electron intensities were convoluted with Gaussian functions with a full width at half maximum (FWHM) of 4.0 eV. Because of large molecular size of MCDS, it was not easy to show correspondence between one of the Auger final-states and a pair of valence orbitals with a hole, as in SiF_4 [37].

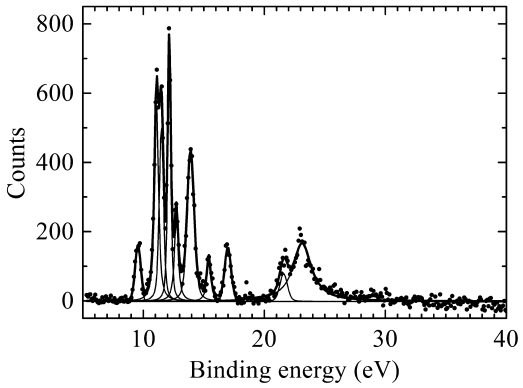

Fig. 1. Valence PES spectrum of MCDS measured at a photon energy of 310.3 eV in the vapor phase. Thin profiles indicate fitting results and a thick curve is the summation of the thin curves.

4. Results and discussion

4.1. Valence PES spectrum

Fig. 1 shows a valence PES spectrum of MCDS vapor measured at a photon energy of 310.3 eV, together with fitting profiles using 11 Voigt functions. The number of valence orbitals in MCDS is 25, judging from the numbers of the constituent atoms and their electrons included. However, 11 profile functions are used for the peak-fitting, because the BE values for some orbitals are very close to one another. Accordingly, some of the fitted peaks correspond to two or three ionic states in Fig. 1, although Fig. 1 shows much finer structures than the spectrum previously obtained in the condensed phase does [12]. In Fig. 1, the peaks in the low BE region would mainly be broadened by vibrational excitation, and those in the high BE region would be broadened by peak overlaps besides. Table 1 lists the measured BE values with their relative peak intensities.

In order to assign the peaks found in the spectrum, a theoretical calculation was carried out by using the OVGF method [13,28]. Table 1 lists the calculated BE values and pole strengths for the valence orbitals together with their assignments. The numbering of the orbital is based on the way that the deepest valence orbital is called 29, because the number of core orbitals in MCDS is 28. The highest occupied molecular orbital (HOMO) is called 53. The main character of each orbital involved in the ionization is expressed by using conventional symbols such as n (non-bonding or lone electron), π and σ [3]. Symbol π_{CH_3} indicates a pseudo π orbital of the CH_3 groups.

Table 1
Experimental and computational BE values of valence electrons in MCDS, together with numbering of the molecular orbitals and their characters. The intensity is normalized to that of the lowest BE peak. Parenthesized digits denote pole strengths.

Experimental		Computational		
BE value (eV)	Intensity	MO number	BE value (eV)	Character
9.6	1.0	53	9.89 (0.91)	σ_{Si-Si}, σ_{Si-C}, n_{Cl}
11.1	3.8	52	11.27 (0.91)	n_{Cl}
		50, 51	11.42 (0.90)	σ_{Si-C}, n_{Cl}
11.5	3.1	48, 49	11.68 (0.91)	n_{Cl}, σ_{Si-C}
12.1	3.3	46, 47	12.32 (0.91)	n_{Cl}
12.7	1.6	45	13.17 (0.91)	σ_{Si-Si}, n_{Cl}, π_{CH_3}
13.9	4.1	44	14.11 (0.91)	π_{CH_3}
		42, 43	14.20 (0.91)	σ_{Si-Cl}, π_{CH_3}
		40, 41	14.45 (0.90)	σ_{Si-Cl}, π_{CH_3}
15.4	0.8	38, 39	14.92 (0.91)	π_{CH_3}, σ_{Si-C}
		37	15.20 (0.91)	σ_{Si-Si}, π_{CH_3}, n_{Cl}
17.0	1.2	36	16.18 (0.89)	σ_{Si-Si}, σ_{Si-Cl}, σ_{Si-C}
18.5	Weak	35	17.92 (0.87)	σ_{Si-Si}, σ_{Si-Cl}, σ_{Si-C}
21.6	0.8			
23.1	5.6			

The peak assignments were mainly made on the basis of closeness between the experimental and computational BE values. The peak intensities experimentally obtained were also used in the assignments, because the high energy photon used here (310.3 eV) induces all the valence ionizations without threshold effects. The computational BE values are close to the measured ones as a whole below 19 eV, where the shallow valence orbitals are positioned. The ionic states at 21.6 and 23.1 eV are composed of complex configurations including some terms of two electrons excitation owing to strong correlation effects in the deep valence orbitals. Accordingly, the assignments of those two peaks are very difficult.

4.2. Si:1s, 2s and 2p core-level PES spectra

Fig. 2a–c respectively show Si:1s, 2s and 2p PES spectra of MCDS measured at photon energies of 1950.8, 350.3 and 320.3 eV. The measured BE values are listed with the computational ones in Table 2, which also includes the measured values of TMS and TCS reported previously [19,38–41].

The Si:1s PES spectrum (Fig. 2a) represents two peaks with nearly the same intensities at 1846.9 and 1849.2 eV, and the two peaks originate from the Si[Me]:1s and Si[Cl]:1s ionizations, respectively [20]. The computational BE values of the Si[Me]:1s and Si[Cl]:1s electrons are much less than the experimental ones in MCDS, although the computational BE difference between the Si[Me]:1s and Si[Cl]:1s electrons is close to the experimental one. The reduction in computational Si:1s BE value from the experimental one mainly comes from relativistic effects [34,42].

The BE value of the Si:1s electron in TMS (1846.3 eV) [19] is less than that in TCS (1850.7 eV) [38]. Similarly, the BE value of the Si[Me]:1s electron (1846.9 eV) is less than that of Si[Cl]:1s (1849.2 eV) in MCDS (Table 2). This variation in BE value is reasonable in view of electronic properties of these three molecules. The CH_3 and Cl ligands have electron-donating and -accepting properties, respectively (Scheme 1). In other words, the electronegativity of the Cl ligand is higher than that of the CH_3 ligand, and then the properties of the ligands increase and decrease the BE values of the Si:1s electrons in TCS and TMS, respectively [1]. As a result, the BE value of the Si:1s electron in TCS becomes larger than that in TMS. Similarly, the BE value of the Si[Cl]:1s electron is larger than that of Si[Me]:1s in MCDS.

On the other hand, the BE value of the Si[Me]:1s electron in MCDS (1846.9 eV) is larger than that of the Si:1s electron in TMS (1846.3 eV), while the BE value of Si[Cl]:1s in MCDS (1849.2 eV) is less than that of Si:1s in TCS (1850.7 eV). This variation in BE value is also reasonable in view of electronic properties of these three molecules. The $-Si(CH_3)_3$ and $-SiCl_3$ moieties have electron-donating and -accepting properties, respectively, and then inter-site electron migration occurs from $-Si(CH_3)_3$ to $-SiCl_3$ in MCDS [43]. As shown in Scheme 1, the inter-site electron migration has an effect opposite to those due to the CH_3 and Cl ligands in MCDS. As a result, the BE value of the Si[Me]:1s electron in MCDS increases and becomes larger than that of Si:1s in TMS, while the value of Si[Cl]:1s decreases and becomes less than that of Si:1s in TCS.

The above-mentioned change in Si:1s BE value on going from TCS to MCDS (1.5 eV) is larger than that from TMS to MCDS (0.6 eV). The reason for this may be explained in the following way. If we pay attention only to atoms directly bonding to the core-ionized Si atom, a halogen atom (Cl) is replaced by a carbon-group element atom (Si) on going from TCS to MCDS, while two carbon-group element atoms (C and Si) are merely exchanged on going from TMS to MCDS. Although the carbon-group element atoms (Si and C) bond to some atoms or groups (H, Cl or CH_3) besides, it is assumed that its bonding does not very largely affect the Si:1s BE values

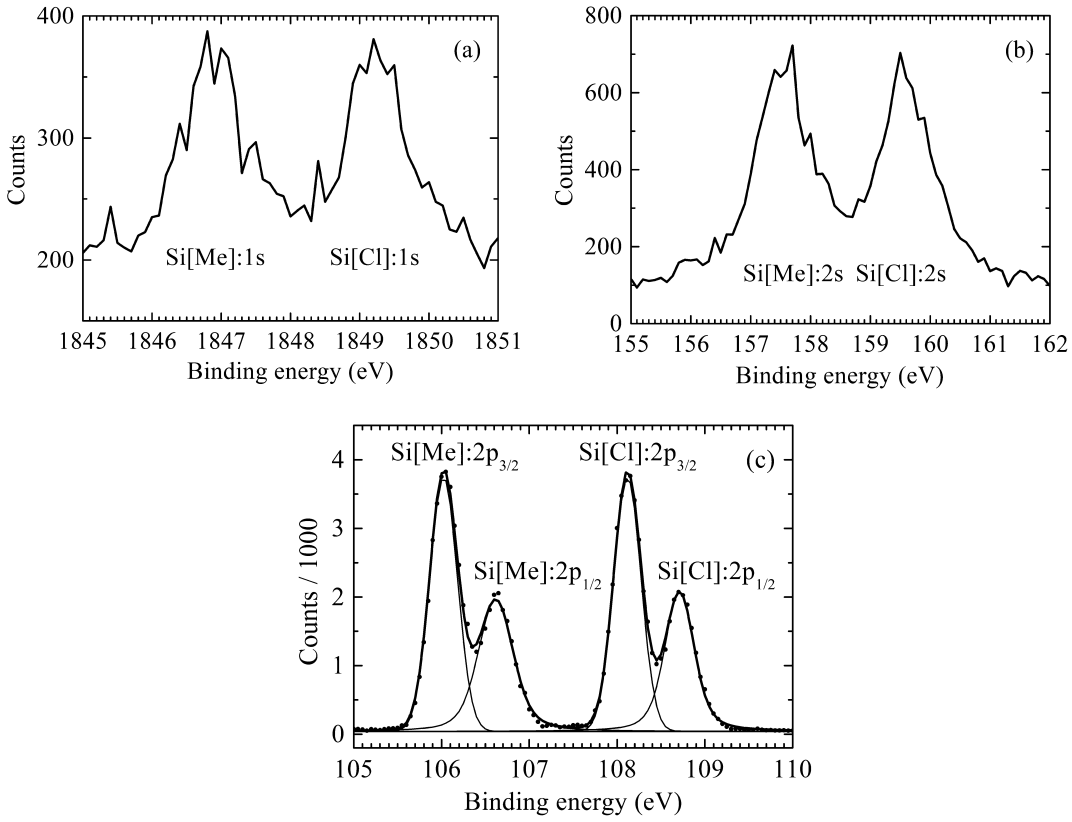

Fig. 2. (a) Si:1s PES spectrum of MCDS measured at a photon energy of 1950.8 eV in the vapor phase. (b) Si:2s PES spectrum at 350.3 eV. (c) Si:2p PES spectrum at 320.3 eV. Thin profiles indicate fitting results and a thick curve is the summation of the thin curves.

in question because of long distances from the core-ionized Si atom to H, Cl or CH_3. Then, it would be reasonable that the BE change on going from TCS to MCDS is larger than that from TMS to MCDS.

Characteristics of the BE values of the Si:2s electrons in MCDS, TCS and TMS [39,40] are close to those of the Si:1s electrons (Table 2). The computational BE values of the Si[Me]:2s and Si[Cl]:2s electrons are much less than the experimental ones in MCDS,

Table 2
Experimental and computational BE values of core electrons in MCDS, together with the experimental ones in TCS and TMS. Intensity ratios between $2p_{1/2}$ and $2p_{3/2}$ photoelectron peaks are given in the parentheses. BE differences between Si[Cl] and Si[Me] sites are given in the brackets.

MCDS	Experimental BE values (eV)	Computational BE values (eV)	Related molecules	Experimental BE values (eV)
Si:1s				
Si[Cl]:1s	1849.2	1843.0	TCS	1850.7[a]
Si[Me]:1s	1846.9	1840.9	TMS	1846.3[b]
	[2.3]	[2.1]		
Si:2s				
Si[Cl]:2s	159.5	150.7	TCS	161.5[c]
Si[Me]:2s	157.6	148.8	TMS	157.1[d]
	[1.9]	[1.9]		
Si:2p				
Si[Cl]:$2p_{1/2}$	108.7 (1.4)	108.0	TCS	110.78[c]
Si[Cl]:$2p_{3/2}$	108.1 (2.0)	108.0	TCS	110.17[c]
Si[Me]:$2p_{1/2}$	106.6 (1.5)	106.0	TMS	106.66[e]
Si[Me]:$2p_{3/2}$	106.0 (2.0)	106.0	TMS	106.04[e]
	[2.1]	[2.0]		
Cl				
1s		2816.6	TCS	2830.4[f]
2s	276.8	291.2	TCS	277.4[a]
$2p_{1/2}$	207.4 (1.2)	205.5	TCS	208.5[c]
$2p_{3/2}$	205.8 (2.0)	205.5	TCS	206.9[c]
C				
1s	290.0	290.3	TMS	289.78[g]

[a] Ref. [38].
[b] Ref. [19].
[c] Ref. [40].
[d] Ref. [39].
[e] Ref. [41].
[f] Ref. [47].
[g] Ref. [46].

although the computational BE difference between the Si[Me]:2s and Si[Cl]:2s electrons is again close to the experimental one. Takahashi and co-workers previously discussed numerical precision of computational BE values for Si:2s orbitals in some Si-containing molecules [42]. Those BE values obtained by means of the DFT method were underestimated by about 10 eV because of inefficient electron correlation included in the calculations. This underestimation could be canceled with the aid of an advanced ab initio molecular-orbital-method such as the complete-active-space self-consistent-field method (CASSCF). However, MCDS is so large in molecular size that the CASSCF method cannot be applied to the BE calculation under the present computational resources.

The Si:2p PES spectrum of MCDS shows two peak groups originating from the Si[Me]:2p and Si[Cl]:2p ionizations around 106 and 108 eV, respectively (Fig. 2c). The splitting between the two peak groups (2.1 eV) is close to that seen in the condensed phase (2.2 eV [43]). The computational BE values of the Si[Me]:2p and Si[Cl]:2p electrons are close to the experimental ones (Table 2). The two peak groups originating from the Si[Me]:2p and Si[Cl]:2p ionizations are further split into two components, which come from the spin–orbit splitting ($2p_{1/2}$ and $2p_{3/2}$).

The BE values of the Si[Cl]:$2p_{1/2}$ and $2p_{3/2}$ electrons in MCDS (108.7 and 108.1 eV) are less than those of Si:$2p_{1/2}$ and $2p_{3/2}$ in TCS (110.78 and 110.17 eV) [40]. This variation is the same as the instances of the Si:1s and 2s electrons. However, the BE values of the Si[Me]:$2p_{1/2}$ and $2p_{3/2}$ electrons (106.6 and 106.0 eV) in MCDS are similar to those of Si:$2p_{1/2}$ and $2p_{3/2}$ in TMS (106.66 and 106.04 eV) [41]. Similarly to the case of the Si:1s ionization, the change in Si:2p BE value on going from TCS to MCDS is larger than that from TMS to MCDS.

The intensity ratios between the $2p_{1/2}$ and $2p_{3/2}$ peaks of MCDS (Table 2) are slightly different from that estimated on the basis of the statistical concept (1:2). The photon energy and detection direction here used might not be appropriate. Accumulation of the experimental data at the magic angle and at a different photon energy may reduce the difference from the intensity ratio estimated on the basis of the statistical concept.

The BE differences between the Si[Me] and Si[Cl] sites in MCDS (2.3, 1.9 and 2.1 eV for Si:1s, 2s and 2p orbitals, respectively, Table 2) are less than those between Si[Me] and Si[F] in FSMSE (3.9, 3.1 and 3.41 eV [13]). The Si:2p BE difference in MCDS is also less than that in CSMSE (2.8 eV [10]). The above-mentioned inter-site electron migration from $-Si(CH_3)_3$ to $-SiCl_3$ decreases the BE differences in MCDS, and the direct bonding between the Si[Me] and Si[Cl] sites reduces site-discrimination.

As shown in Table 2, the experimental and computational BE differences between the Si[Me] and Si[Cl] sites in MCDS decrease in the order 1s > 2p > 2s. This order in BE difference is the same as that in FSMSE [9,13], and the reason for the order 1s > 2p (2s) was previously explained in terms of differences in principal quantum number and effective nuclear charge between the 1s and 2p (2s) orbitals [44]. The Si:1s ionization thus gives slightly better site-discrimination than the Si:2p (2s) ionization under common experimental conditions concerning energy resolution. If specific experimental difficulties for the Si:1s ionization [45] are neglected, the better site discrimination in the Si:1s ionization will potentially make site selection clearer.

4.3. Cl:2s and 2p core-level PES spectra

Fig. 3 shows Cl:2s and 2p PES spectra of MCDS. As shown in Table 2, the computational BE value of the Cl:2p electron is similar to the experimental one, though the computational value of Cl:2s is much larger than the experimental one. The spin-orbit splitting between Cl:$2p_{1/2}$ and $2p_{3/2}$ in MCDS, 1.6 eV, is the same as that in TCS [40,46]. The intensity ratio of this splitting is similar to the statistical weight (1:2). The photons provided by the beamline used here cannot ionize the Cl:1s electron of MCDS, although the Cl:1s BE value of TCS was reported previously [47].

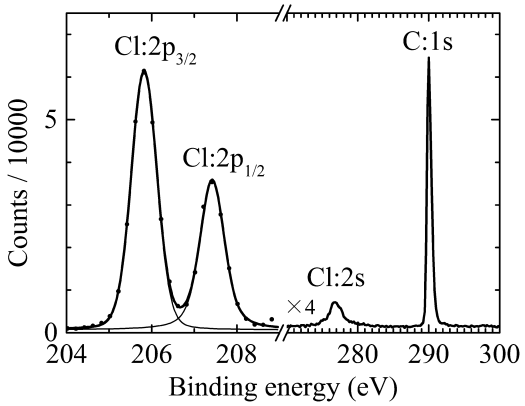

Fig. 3. Cl:2s, 2p and C:1s PES spectra of MCDS in the vapor phase. The Cl:2p PES spectrum was measured at a photon energy of 430.0 eV. Thin profiles indicate fitting results and a thick curve is the summation of the thin curves. The Cl:2s and C:1s PES spectra were measured at a photon energy of 325.0 eV.

As listed in Table 2, the BE values of the Cl:2s and 2p electrons in MCDS are less than those in TCS [38,40] by 0.6 and 1.1 eV, respectively. Since a $-Si(CH_3)_3$ group has an electron-donating property, electron-accepting capacity of a $-SiCl_2Si(CH_3)_3$ group in MCDS is less than that of a $-SiCl_3$ group in TCS. In other words, the electronegativity of the $-SiCl_2Si(CH_3)_3$ group in MCDS is lower than that of the $-SiCl_3$ group in TCS, and then the Cl atom bonding to the $-SiCl_2Si(CH_3)_3$ group in MCDS shows a smaller 2s (2p) BE value than the Cl atom bonding to $-SiCl_3$ in TCS does [1].

The reason why the Cl:2s BE difference between MCDS and TCS (0.6 eV) is less than the Cl:2p BE difference (1.1 eV) can be explained in the following way. In a simple physical picture, applicable to many-electron atoms [48], the BE value, $I_{X,Y}$, of the Cl:Y electron (Y = 2s or 2p) in X molecule (X = MCDS or TCS) is given by

$$I_{X,Y} = \frac{R \cdot Z^{*2}_{X,Y}}{n^2} \quad (1)$$

where R = 13.6 eV, n = 2 and $Z^*_{X,Y}$ denotes the effective nuclear charge divided by the elementary charge (e). The $Z^*_{X,Y}$ value is less than 17 (atomic number of Cl), because the Cl:Y electron in MCDS and TCS experiences a Coulombic repulsion due to the presence of all other electrons. If the Cl:Y electron is at a distance r_Y from the corresponding Cl nucleus, it experiences a repulsion that can be approximately represented by a negative point charge located at the Cl nucleus. This charge is equal in magnitude to the total charge of the electrons within a sphere of radius r_Y [49]. This point negative charge reduces the full positive charge of the Cl nucleus from $17e$ to $eZ^*_{X,Y}$, and the Cl:Y electron experiences the shielded nuclear charge; that is, the shielding experienced by the Cl:Y electron is proportional to $(17 - Z^*_{X,Y})$.

A Cl:2s electron is more likely to be found (penetrate) close to the Cl nucleus than a Cl:2p electron [49]. In other words, there is a high probability of $r_{2s} < r_{2p}$, and so the Cl:2s electron generally experiences less shielding than the Cl:2p electron ($17 - Z^*_{X,2s} < 17 - Z^*_{X,2p}$) [49]. Therefore, $17 > Z^*_{X,2s} > Z^*_{X,2p}$, and $I_{X,2s} > I_{X,2p}$ (Table 2) according to Eq. (1).

A part of the shielding due to the above-mentioned negative point-charge comes from valence electrons of X molecule, and induces substituent effects on $Z^*_{X,Y}$ and $I_{X,Y}$. Since the sphere of radius r_{2s} is smaller than the concentric sphere of radius r_{2p}, the substitution-induced change in the negative point charge experienced by the Cl:2s electron is less than that by the Cl:2p electron, and the substituent effect on $Z^*_{X,2s}$ is less than that on $Z^*_{X,2p}$.

Therefore, the change on going from TCS to MCDS has a smaller influence on the $Z^*_{X,2s}$ value than on $Z^*_{X,2p}$ ($Z^*_{TCS,2s} - Z^*_{MCDS,2s} < Z^*_{TCS,2p} - Z^*_{MCDS,2p}$), and the effect on the $I_{X,2s}$ value is also less than that on $I_{X,2p}$ according to Eq. (1); that is, the change on going from TCS to MCDS has a smaller influence on the Cl:2s BE value than on the Cl:2p BE value.

This explanation is very simple but consistent with the present experimental result that the Cl:2s BE difference between TCS and MCDS is less than the Cl:2p BE difference. The Si:2s BE difference between the Si[Cl] and Si[Me] sites in MCDS is also less than the Si:2p BE difference as shown in Section 4.2, which can be explained similarly. Previous explanation given for a similar BE difference between Si[F] and Si[Me] in FSMSE (Si:2s < Si:2p) in Ref. [44] should be revised.

4.4. C:1s core-level PES spectrum

Fig. 3 also shows a C:1s PES spectrum of MCDS. As shown in Table 2, the computational BE value of the C:1s electron is close to the experimental one. The C:1s BE value of MCDS obtained in the present study is larger than that of TMS [46] by 0.2 eV. Since a $-SiCl_3$ group has an electron-accepting property, electronegativity of a $-Si(CH_3)_2SiCl_3$ group in MCDS is higher than that of a $-Si(CH_3)_3$ group in TMS, and then the C atom bonding to the $-Si(CH_3)_2SiCl_3$ group in MCDS shows a larger 1s BE value than the C atom bonding to $-Si(CH_3)_3$ in TMS [1].

4.5. Normal AES spectra

Resonant and normal Si:$KL_{23}L_{23}$ AES spectra of MCDS were reported previously [20]. Fig. 4a shows an experimental normal Si:L_{23}VV AES spectrum of MCDS measured at a photon energy of 335.0 eV. This spectrum is called singles Si:L_{23}VV AES spectrum [50]. Fig. 4b and c respectively show computational AES spectra after creation of Si[Cl]:2p and Si[Me]:2p core holes in MCDS, and correspond to the Si:L_{23}VV-Si[Cl]:2p and Si:L_{23}VV-Si[Me]:2p Auger photoelectron coincidence spectra (APECS spectra) [50]. Fig. 4d shows the summation of the spectra given in panels (b) and (c). The computational spectrum given in panel (d) corresponds to the experimental one in panel (a). Fig. 4e and f show experimental normal Si:L_{23}VV AES spectra of TCS and TMS, respectively.

The computational Si[Cl]:L_{23}VV AES spectrum (Fig. 4b) has three peaks at 74, 57 and 47 eV together with a small peak around 65 eV. The highest kinetic-energy peak at 74 eV is accompanied by a small shoulder around 81 eV. The computational Si[Me]:L_{23}VV AES spectrum (Fig. 4c) has two peaks at 76 and 66 eV together with small peaks around 82, 60 and 49 eV. As reported previously [51], a normal Auger electron emitted from a shallow valence orbital generally has large kinetic energy, and the normal Auger transition is often localized around the core-ionized atomic site. Accordingly, the Si[Cl]:L_{23}VV Auger electron emission with large kinetic energy mainly yields doubly charged states with two holes in the Cl lone-pair orbitals (MO numbers 52, 47 and so forth in Table 1) or with one hole in the Cl lone-pair orbital and another in a shallow valence orbital (MO number 53 and so forth). The Si[Me]:L_{23}VV Auger electron emission with large kinetic energy mainly yields doubly charged states with two holes in the HOMO (MO number 53) or with one hole in the HOMO and another in a shallow orbital (MO number 51 and so forth).

A normal Auger-electron kinetic-energy (E_a) released through two valence-holes creation is often written in the following way [14,17].

$$E_a = I_c - I_{v1} - I_{v2} - I_{hh} \quad (2)$$

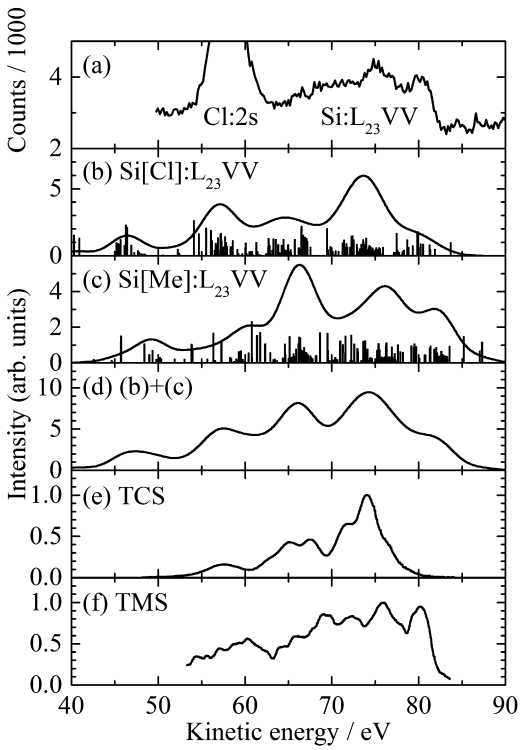

Fig. 4. Normal Si:L_{23}VV AES spectra. (a) Experimental spectrum of MCDS measured at a photon energy of 335.0 eV in the vapor phase. The structures below 63 eV overlap with the Cl:2s photoelectron peak, and the structure around 85 eV probably corresponds to a Cl:2p photoelectron satellite structure. (b) Computational spectrum after creation of a Si[Cl]:2p core hole in MCDS. The line spectrum shows Auger electron intensities for singlet Si[Cl]:L_{23}VV-Auger final-states after creation of a Si[Cl]:2p core hole. The curve indicates the result of Gaussian convolution (FWHM = 4.0 eV) of the Auger electron intensities for all the singlet and triplet Si[Cl]:L_{23}VV-Auger final-states. (c) Computational line and convolution spectra after creation of a Si[Me]:2p core hole in MCDS. (d) Summation of the convolution spectra shown in panels (b) and (c). This computational spectrum corresponds to the experimental one shown in panel (a). (e) Experimental spectrum of TCS vapor [15]. (f) Experimental spectrum of TMS vapor [16].

Here I_c denotes the BE value for the core orbital, I_{v1} and I_{v2} are those for the valence orbitals, and I_{hh} means the effective hole–hole interaction energy. When an Auger-decay yields two holes at one atom, I_{hh} becomes very large. When another decay forms two holes in one or two delocalized valence-orbitals, I_{hh} decreases considerably. The magnitude of the hole–hole interaction represents a character of the valence holes and a feature of spatial overlapping between the relevant orbitals, and is an interesting point in investigation of AES spectra.

The experimental normal Si:L_{23}VV AES spectrum of MCDS in panel (a) consists of two components, Auger electron emissions from the Si[Me] and Si[Cl] sites. Note that the structures below 63 eV overlap with the Cl:2s photoelectron peak and that the structure around 85 eV probably corresponds to a Cl:2p photoelectron satellite structure. The experimental spectrum given in panel (a) is similar to the computational spectrum in panel (d). Accordingly, the peak at 80 eV in the experimental spectrum is supposed to come from the Si[Me]:L_{23}VV Auger decays yielding doubly charged states with two holes in the HOMO (MO number 53) or with one hole in the HOMO and another in a shallow valence orbital (MO number 51 and so forth). In the doubly charged states (Auger final-states), the I_{hh} value in Eq. (2) is relatively small (about 8 eV) because the two holes are delocalized over the molecule. On the other hand, the peak at 75 eV is assigned to doubly charged states with two holes in the Cl lone-pair orbitals (MO numbers 52, 47 and so forth) or with one hole in the Cl lone-pair orbital and another in a shallow valence

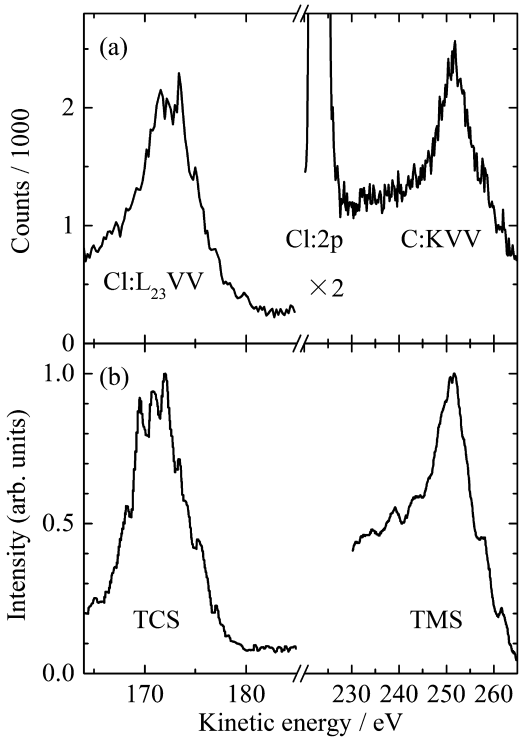

Fig. 5. (a) Normal Cl:L_{23}VV and C:KVV AES spectra of MCDS measured at photon energies of 320.0 and 430.0 eV, respectively, in the vapor phase. In the Cl:L_{23}VV AES spectrum, the tail to the lower kinetic-energy side below 165 eV overlaps with the Si:2s photoelectron peaks. In the C:KVV AES spectrum, the tail to the lower energy side below 230 eV overlaps with the Cl:2p photoelectron peaks. (b) Normal AES spectra of TCS and TMS vapors [15,16].

orbital (MO number 53 and so forth). Then, the I_{hh} value is relatively large (about 10 eV) because of the hole localization around the Cl atoms. The shoulder around 70 eV probably comes from both the Si[Me]:L_{23}VV and Si[Cl]:L_{23}VV Auger-decays.

Further it can be said that the experimental AES spectrum of MCDS (panel (a)) is approximately formed from a superposition of those of TMS and TCS (panels (e) and (f)) [15,16]. The APECS measurements may throw more light on this problem.

Judging from the above-mentioned results, just after the Si[Me]:L_{23}VV and Si[Cl]:L_{23}VV Auger-decays, MCDS seems to remember the Si site where the core ionization has taken place, although site-discrimination in the core ionization is somewhat reduced on going from FSMSE (and CSMSE) to MCDS as described in Section 4.2. However, ionic fragmentations induced by the Si[Me]:2p and Si[Cl]:2p ionizations are similar to each other in MCDS [10,12], in contrast to those in FSMSE and CSMSE where site-specific fragmentations are revealed [8,10,11]. During the ionic fragmentations, MCDS forgets the core-ionized Si site, although FSMSE and CSMSE still remember it. The reason for this can be explained in terms of the difference in valence-hole's spatial-distribution between MCDS and FSMSE (CSMSE). The spatial distributions of the valence holes created through the Si[Me]:L_{23}VV and Si[Cl]:L_{23}VV Auger decays in MCDS would significantly overlap with each other owing to the direct Si—Si bonding. Accordingly, in the Si[Me]:2p and Si[Cl]:2p ionizations, the valence holes weaken the same chemical bonds. Then, the $MCDS^{2+}$ turns into several ionic fragments through various dissociation channels. As a result, the ionic fragmentations induced by the Si[Me]:2p and Si[Cl]:2p ionizations are similar to each other. In contrast, since the two Si sites in each of FSMSE and CSMSE are separated by a dimethylene group, the overlap of the spatial-distributions of the valence holes is not extensive, and thus the ionic fragmentations occur selectively around the Si site where the core ionization has taken place.

On the basis of speculation we have given the reason for the difference in fragmentation pattern between MCDS and FSMSE (CSMSE). Although it is important to show the spatial distribution of the valence holes created through the Auger decays, the spatial distribution is being discussed in another publication because of its complexity in these large molecules.

A Cl:L_{23}VV AES spectrum of MCDS measured at 320.0 eV is shown in Fig. 5a, which exhibits a profile close to that of TCS (Fig. 5b) [15]. The highest peak at 173 eV, together with the tail to the higher kinetic-energy side, would mainly be generated through Auger decays forming doubly charged states with two holes in the Cl lone-pair orbitals (MO numbers 52, 47 and so forth) or with one hole in the Cl lone-pair orbital and another in a shallow valence orbital (MO number 53 and so forth). In the doubly charged states, the I_{hh} value is large (about 11 eV) because of the hole localization around the Cl atoms. The emissions below 170 eV would mainly originate from doubly charged states with a deep valence hole and a shallow valence hole. The tail to the lower energy side below 165 eV overlaps with the Si:2s photoelectron peaks.

A C:KVV AES spectrum of MCDS measured at 430.0 eV is also shown in Fig. 5a, which exhibits a profile close to that of TMS (Fig. 5b) [16]. Estimation of the I_{hh} value for the highest peak at 252 eV is difficult because a lot of valence orbitals concern the Auger final-states. The tail to the lower energy side below 230 eV overlaps with the Cl:2p photoelectron peaks.

5. Summary

Various PES and AES spectra of MCDS were measured by means of an electron energy analyzer combined with monochromatized undulator radiation. The measured spectra were interpreted with the aid of some calculations by means of the OVGF or DFT method. Since MCDS consists of —$SiCl_3$ and —$Si(CH_3)_3$ moieties, the core-electron BE values obtained experimentally were compared with those of TCS and TMS. This comparison showed that electronic properties of MCDS hold a close correlation with those of TCS and TMS, although the direct Si—Si bonding reduces site-discrimination in MCDS. A similar correlation was found in the Auger decays. Although the Si:L_{23}VV Auger final-states of MCDS might remember the Si site where the core ionization has taken place, this memory disappears in the subsequent ionic fragmentations. In order for site-specific fragmentation to be revealed, an atomic site of interest must be separated by a dimethylene group (about 5 Å) from any other atomic site around which bond cleavage is undesirable. If not, bond dissociation occurs not only around the target site but also around the undesirable site. The present findings provide fundamental data on energy levels of MCDS as well as on the electronic structures. The outcomes here obtained would stimulate more precise studies on electronic structures and dynamical behaviors of Si-containing molecules.

Acknowledgments

The authors wish to express their sincere thanks to Mr. Tsunagu Mochizuki and Dr. Takuhiro Kakiuchi of Ehime University, Dr. Hironobu Fukuzawa, Mr. Tetsuya Tachibana and Mr. Syuhei Yamada of Tohoku University for their assistance in a part of the experiments and analyses. The authors are also indebted to Professor Joji Ohshita of Hiroshima University for his generously providing us with MCDS. S.N. thanks Dr. Umpei Nagashima of National Institute of Advanced Industrial Science and Technology for his valuable discussion. I.H.S. expresses his appreciation for support by Dr. Masaki Koike of AIST during this study. This research

was carried out with the approval of the SPring-8 Program Advisory Committee (Proposal Nos. 2012A1067 and 2013A1045). The computations were performed at Research Center for Computational Science, Okazaki, Japan and Information Media Center of Hiroshima University, Higashi-Hiroshima, Japan.

Appendix A. Supplementary data

Supplementary data associated with this article can be found, in the online version, at http://dx.doi.org/10.1016/j.elspec.2014.04.009.

References

[1] K. Siegbahn, C. Nordling, G. Johansson, J. Hedman, P.F. Hedén, K. Hamrin, U. Gelius, T. Bergmark, L.O. Werme, R. Manne, Y. Baer, ESCA Applied to Free Molecules, North-Holland, Amsterdam, 1969, pp. 156–163.
[2] D.W. Turner, C. Baker, A.D. Baker, C.R. Brundle, Molecular Photoelectron Spectroscopy, John Wily Sons, London, 1970.
[3] K. Kimura, S. Katsumata, Y. Achiba, T. Yamazaki, S. Iwata, Handbook of HeI Photoelectron Spectra of Fundamental Organic Molecules, Japan Scientific Societies Press/Halsted Press, Tokyo/New York, 1981.
[4] S. Nagaoka, J. Chem. Educ. 84 (2007) 801–802.
[5] D. Céolin, C. Miron, K. Le Guen, R. Guillemin, P. Morin, E. Shigemasa, P. Millié, M. Ahmad, P. Lablanquie, F. Penent, M. Simon, J. Chem. Phys. 123 (2005) 234303 (8 pp.).
[6] R. Guillemin, W.C. Stolte, D.W. Lindle, J. Phys. B 42 (2009) 125101 (7 pp.).
[7] I.H. Suzuki, N. Saito, J.D. Bozek, J. Electron Spectrosc. Relat. Phenom. 101–103 (1999) 69–73.
[8] S. Nagaoka, G. Prümper, H. Fukuzawa, M. Hino, M. Takemoto, Y. Tamenori, J. Harries, I.H. Suzuki, O. Takahashi, K. Okada, K. Tabayashi, X.-J. Liu, T. Lischke, K. Ueda, Phys. Rev. A 75 (2007) 020502(R) (4 pp.).
[9] S. Nagaoka, M. Takemoto, G. Prümper, H. Fukuzawa, Y. Tamenori, I.H. Suzuki, K. Ueda, J. Chem. Phys. 129 (2008) 204309 (7 pp.).
[10] S. Nagaoka, H. Fukuzawa, G. Prümper, M. Takemoto, O. Takahashi, K. Yamaguchi, T. Kakiuchi, K. Tabayashi, I.H. Suzuki, J.R. Harries, Y. Tamenori, K. Ueda, J. Phys. Chem. A 115 (2011) 8822–8831.
[11] S. Nagaoka, K. Mase, M. Nagasono, S. Tanaka, T. Urisu, J. Ohshita, J. Chem. Phys. 107 (1997) 10751–10755.
[12] S. Nagaoka, K. Mase, M. Nagasono, S. Tanaka, T. Urisu, J. Ohshita, U. Nagashima, Chem. Phys. 249 (1999) 15–27.
[13] I.H. Suzuki, A. Nitta, A. Shimizu, Y. Tamenori, H. Fukuzawa, K. Ueda, S. Nagaoka, J. Electron Spectrosc. Relat. Phenom. 173 (2009) 18–23.
[14] S. Nagaoka, A. Nitta, Y. Tamenori, H. Fukuzawa, K. Ueda, O. Takahashi, T. Kakiuchi, Y. Kitajima, K. Mase, I.H. Suzuki, J. Electron Spectrosc. Relat. Phenom. 175 (2009) 14–20.
[15] S. Aksela, O.-P. Sairanen, H. Aksela, G.M. Bancroft, K.H. Tan, Phys. Rev. A 37 (1988) 2934–2940.
[16] G.G.B. de Souza, R. Platania, A.C. de, A.E. Souza, F. Maracci, Chem. Phys. 129 (1989) 491–494.
[17] I.H. Suzuki, A. Nitta, H. Fukuzawa, K. Ueda, O. Takahashi, Y. Tamenori, S. Nagaoka, J. Chem. Phys. 131 (2009) 164309 (8 pp.).
[18] I.H. Suzuki, Y. Kono, A. Ikeda, T. Ouchi, K. Ueda, O. Takahashi, I. Higuchi, Y. Tamenori, S. Nagaoka, Phys. Rev. A 82 (2010) 045401 (4 pp.).
[19] I.H. Suzuki, Y. Kono, A. Ikeda, T. Ouchi, K. Ueda, O. Takahashi, I. Higuchi, Y. Tamenori, S. Nagaoka, J. Chem. Phys. 134 (2011) 084312 (7 pp.).
[20] I.H. Suzuki, H. Endo, K. Nagai, O. Takahashi, Y. Tamenori, S. Nagaoka, J. Chem. Phys. 139 (2013) 174314 (7 pp.).
[21] S. Nagaoka, J. Ohshita, M. Ishikawa, T. Masuoka, I. Koyano, J. Phys. Chem. 97 (1993) 1488–1495.
[22] H. Ohashi, E. Ishiguro, Y. Tamenori, H. Kishimoto, M. Tanaka, M. Irie, T. Tanaka, T. Ishikawa, Nucl. Instrum. Methods A 467–468 (2011) 529–532.
[23] Y. Tamenori, H. Ohashi, E. Ishiguro, T. Ishikawa, Rev. Sci. Instrum. 73 (2002) 1588–1590.
[24] V. Schmidt, Electron Spectrometry of Atoms using Synchrotron Radiation, Cambridge University Press, Cambridge, 1997 (Chapter 6).
[25] K. Okada, M. Kosugi, A. Fujii, S. Nagaoka, T. Ibuki, S. Samori, Y. Tamenori, H. Ohashi, I.H. Suzuki, K. Ohno, J. Phys. B 38 (2005) 421–431.
[26] Supplementary material. The geometrical structure of the present molecule, MCDS, is indicated in graphics from three directions and in coordinate data.
[27] M.J. Frisch, et al., Gaussian 09 Revision C.01, Gaussian, Inc., Wallingford, CT, 2010.
[28] A. Szabo, N.S. Ostlund, Modern Quantum Chemistry, Macmillan, London, 1982 (Chapter 7).
[29] EPT, in: Gaussian 09 User's Reference, http://www.gaussian.com/g_tech/g_ur/k_ept.htm (accessed May 2014).
[30] M.R. Estrada, G.N. Zamarbide, J. Sánchez-Marín, An. Asoc. Quim. Argent. 94 (2006) 81–94.
[31] M.S. Deleuze, M.G. Giuffreda, J.-P. François, J. Phys. Chem. A 106 (2002) 5626–5637.
[32] O. Takahashi, K. Yamasaki, S. Nagaoka, K. Ueda, Chem. Phys. Lett. 518 (2011) 44–48.
[33] K. Hermann, et al., StoBe-deMon Version 2.2, 2006.
[34] O. Takahashi, L.G.M. Pettersson, J. Chem. Phys. 121 (2004) 10339–10345.
[35] J.P. Perdew, W. Yue, Phys. Rev. B 33 (1986) 8800–8802, 40 (1989) 3399–3399 (Erratum).
[36] J.P. Perdew, Y. Wang, Phys. Rev. B 45 (1992) 13244–13249.
[37] F.O. Gottfried, L.S. Cederbaum, F. Tarantelli, Phys. Rev. A 53 (1996) 2118–2129.
[38] I.H. Suzuki, Y. Kono, K. Sakai, M. Kimura, K. Ueda, Y. Tamenori, O. Takahashi, S. Nagaoka, J. Phys. B 46 (2013) 075101 (9 pp.).
[39] S.G. Urquhart, J.Z. Xiong, A.T. Wen, T.K. Sham, K.M. Baines, G.G.B. de Souza, A.P. Hitchcock, Chem. Phys. 189 (1994) 757–768.
[40] J.D. Bozek, K.H. Tan, G.M. Bancroft, J.S. Tse, Chem. Phys. Lett. 138 (1987) 33–42.
[41] J.D. Bozek, G.M. Bancroft, K.H. Tan, Phys. Rev. A 43 (1991) 3597–3608.
[42] O. Takahashi, M. Tashiro, M. Ehara, K. Yamasaki, K. Ueda, Chem. Phys. 384 (2011) 28–35.
[43] S. Nagaoka, U. Nagashima, J. Ohshita, Bull. Chem. Soc. Jpn. 79 (2006) 537–548.
[44] U. Nagashima, S. Nagaoka, Bull. Chem. Soc. Jpn. 82 (2009) 1248–1249.
[45] S. Nagaoka, A. Tamura, A. Fujii, J. Ohshita, K. Okada, T. Ibuki, I.H. Suzuki, H. Ohashi, Y. Tamenori, Int. J. Mass Spectrom. 247 (2005) 101–105.
[46] J.E. Drake, C. Riddle, L. Coatsworth, Can. J. Chem. 53 (1975) 3602–3612.
[47] A.W. Potts, H.F. Fhadil, J.M. Benson, I.H. Hillier, Chem. Phys. Lett. 230 (1994) 543–546.
[48] G.C. Pimentel, R.D. Spratley, Chemical Bonding Clarified through Quantum Mechanics, Holden-Day, San Francisco, 1969 (Chapters 1 and 2).
[49] P. Atkins, J. de Paula, Atkins' Physical Chemistry, 9th ed., Oxford University Press, Oxford, 2010 (Section 9.4).
[50] K. Mase, E. Kobayashi, A. Nambu, T. Kakiuchi, O. Takahashi, K. Tabayashi, J. Ohshita, S. Hashimoto, M. Tanaka, S. Nagaoka, Surf. Sci. 607 (2013) 174–180.
[51] S. Nagaoka, S. Tanaka, K. Mase, J. Phys. Chem. B 105 (2001) 1554–1561.